

# Diffusion of Chiral Janus Particles in a Sinusoidal Channel

XUE AO<sup>1</sup>, P. K. GHOSH<sup>2</sup>, Y. LI<sup>3</sup> <sup>(a)</sup>, G. SCHMID<sup>1</sup>, P. HÄNGGI<sup>1,3</sup> and F. MARCHESONI<sup>3,4</sup>

<sup>1</sup> *Institut für Physik, Universität Augsburg, D-86135 Augsburg, Germany*

<sup>2</sup> *Department of Chemistry, Presidency University, Kolkata - 700073, India*

<sup>3</sup> *Center for Phononics and Thermal Energy Science, School of Physics Sciences and Engineering, Tongji University, Shanghai 200092, People's Republic of China*

<sup>4</sup> *Dipartimento di Fisica, Università di Camerino, I-62032 Camerino, Italy*

PACS 82.70.Dd – Colloids  
 PACS 87.15.hj – Transport dynamics  
 PACS 36.40.Wa – Charged clusters

**Abstract** – We investigate the transport diffusivity of artificial microswimmers, a.k.a. Janus particles, moving in a sinusoidal channel in the absence of external biases. Their diffusion constant turns out to be quite sensitive to the self-propulsion mechanism and the geometry of the channel compartments. Our analysis thus suggests how to best control the diffusion of active Brownian motion in confined geometries.

**Introduction.** – Over the last decade the problem of controlling transport of regular Brownian particles in narrow corrugated channels has attracted the attention of many investigators with the purpose of better understanding biological processes in the cell or designing artificial micro- and nano-devices [1, 2]. In a recent development [3] regular Brownian particles have been replaced with a special type of diffusive tracers, namely, with active or self-propelled artificial micro-swimmers. Since such particles operate by harvesting energy from their environment, mostly in a non-equilibrium steady state, their autonomous transport is generally enhanced [3].

Self-propulsion is the ability of most living organisms to move, in the absence of external drives, thanks to an “engine” of their own [4]. Optimizing self-propulsion of micro- and nano-particles (artificial microswimmers) is a growing topic of today’s nanotechnology [5–8]. Recently, a new type of artificial microswimmers has been synthesized [9, 10], where self-propulsion takes advantage of the local gradients asymmetric particles can generate in the presence of an external energy source (self-phoretic effects). Such particles, called Janus particles (JP), consist of two distinct “faces”, only one of which is chemically or physically active. Thanks to their functional asymmetry, JP’s can induce either concentration gradients (self-diffusiophoresis) by catalyzing a chemical reaction on their active surface [11, 12], or thermal gradients (self-

thermophoresis), e.g., by inhomogeneous light absorption [13] or magnetic excitation [14].

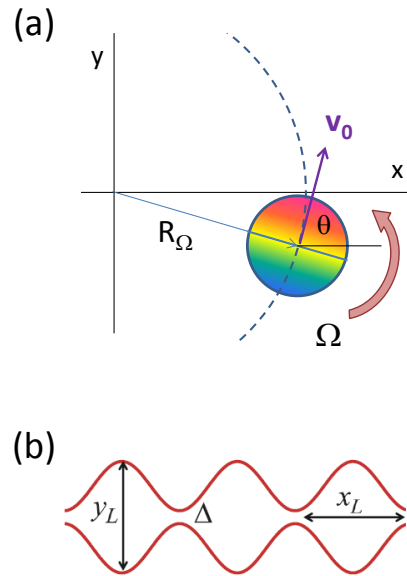


Fig. 1: (Color online) (a) Chiral levogyre Janus particle with  $\Omega > 0$  in the bulk. Sketch of a noiseless particle with self-propulsion velocity  $\mathbf{v}_0$  and finite torque frequency  $\Omega$ , Eq. (1), moving along a circular arc of radius  $R_\Omega$  (dashed line); (b) Sketch of the sinusoidal channel of Eq. (2). Due to its symmetry, this channel does not rectify JP diffusion.

<sup>(a)</sup>E-mail: yunyunli@tongji.edu.cn

A self-propulsion mechanism acts on an pointlike particle by means of a force and, possibly, a torque. In the absence of a torque, the line of motion is directed parallel to the self-phoretic force and the JP propels itself along a straight line, until it changes direction after a mean persistence length,  $l_\theta$ , due to gradient fluctuations [15] or random collisions against other particles or geometric boundaries [16]. In the presence of asymmetries in the propulsion mechanism, the self-phoretic force and the line of motion are no longer aligned and the microswimmer tends to execute circular orbits with radius  $R_\Omega$ , as if subject to a torque with chiral frequency  $\Omega$  [17, 18] (Fig. 1).

Active chiral motion has long been known in biology [18–20] and more recently observed in asymmetrically propelled micro- and nano-rods: A torque can be intrinsic to the propulsion mechanism, due to the presence of geometrical asymmetries in the particle fabrication, engineered or accidental (asymmetric JP’s) [21–23], or externally applied, for instance, by laser irradiation [13] or hydrodynamic fields [24].

Active Brownian motion is time correlated *per se*, which means that rectification of a JP can be easily achieved by choosing spatially asymmetric channel boundaries [3]. As we intend to investigate the interplay of propulsion chirality and geometric confinement on the diffusivity of a channeled JP, here we restrict our analysis to the case of sinusoidal channels, where the rectification current is known to be identically zero, both for passive and active Brownian motion. The extension of the present work to the case of spatially asymmetric channels will be presented in a forthcoming publication [25]. The main results presented below can be summarized as follows: (i) A finite torque,  $|\Omega| > 0$ , tends to suppress the particle diffusivity even in the bulk, according to a simple phenomenological law that fits remarkably well the simulation data. This effect grows prominent for chiral radii much shorter than the self-propulsion length,  $R_\Omega \ll l_\theta$ ; (ii) The diffusivity of channeled microswimmers, besides decreasing with  $|\Omega|$  as in the bulk, exhibits an additional side peak, which corresponds to the optimal condition, when a channel compartment can accommodate for a closed orbit of the chiral swimmer, thus trapping it; (iii) These properties are rather sensitive to both the self-propulsion mechanism of the microswimmer and the geometry of the channel, which points to simple techniques for sorting out microswimmers according to their swimming properties.

**Model.** – In order to avoid unessential complications, we restrict our analysis to the case of 2D channels and pointlike artificial microswimmers of the JP type [9]. The extension of our conclusions to 3D channels and finite-size particles [26] is straightforward. A chiral JP gets a continuous push from the suspension fluid, which in the overdamped regime amounts to a rotating self-propulsion velocity  $\mathbf{v}_0$  with constant modulus  $v_0$  and angular velocity  $\Omega$ . Additionally, the self-propulsion direction varies randomly with time constant  $\tau_\theta$ , under the combined action

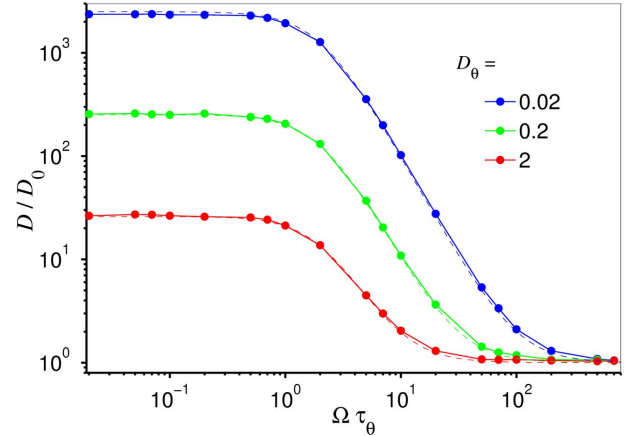


Fig. 2: (Color online) Diffusion of a levogyre JP with  $\Omega \geq 0$  and  $v_0 = 1$  in a straight channel:  $D_{\text{ch}}$  vs.  $\Omega$  for different  $D_\theta$  and  $D_0 = 0.01$ . The boundaries  $w_\pm(x)$  are given by Eq. (2) with  $\Delta = y_L = 1$ . The dashed curves represent the corresponding phenomenological law,  $D_{\text{ch}} = D$ , holding for straight channels, with  $D$  given in Eq. (7). Our results are independent on the sign of  $\Omega$  and the width of the straight channel (not shown).

of thermal noise and orientational fluctuations intrinsic to the self-propulsion mechanism.

The bulk dynamics of such an overdamped chiral JP obeys the Langevin equations [17, 20, 27]

$$\begin{aligned} \dot{x} &= v_0 \cos \theta + \xi_x(t) \\ \dot{y} &= v_0 \sin \theta + \xi_y(t) \\ \dot{\theta} &= \Omega + \xi_\theta(t), \end{aligned} \quad (1)$$

where the coordinates of the particle center of mass,  $\mathbf{r} = (x, y)$ , are subject to the Gaussian noises  $\xi_i(t)$ , with  $\langle \xi_i(t) \rangle = 0$  and  $\langle \xi_i(t) \xi_j(0) \rangle = 2D_0 \delta_{ij} \delta(t)$  for  $i = x, y$ , modeling the equilibrium thermal fluctuations in the suspension fluid. The channel is directed along the  $x$  axis, the self-propulsion velocity is oriented at an angle  $\theta$  with respect to it and the sign of  $\Omega$  is chosen so as to coincide respectively with the positive (levogyre) and negative (dextrogyre) chirality of the swimmer, see Fig. 1. The orientational fluctuations of the propulsion velocity are modeled by the Gaussian noise  $\xi_\theta(t)$  with  $\langle \xi_\theta(t) \rangle = 0$  and  $\langle \xi_\theta(t) \xi_\theta(0) \rangle = 2D_\theta \delta(t)$ , where, as shown below,  $D_\theta$  sets the orientational time constant,  $\tau_\theta$ , of the self-propulsion velocity,  $\tau_\theta = 2/D_\theta$ . Accordingly, the microswimmer mean free self-propulsion path approximates a circular arc of radius  $R_\Omega = v_0/|\Omega|$  and length  $l_\theta = v_0 \tau_\theta$  [17]. Therefore, for  $R_\Omega \lesssim l_\theta$ , or equivalently,  $|\Omega| \tau_\theta \gtrsim 1$  (strong chirality regime), chiral effects tend to appreciably suppress the ensuing active Brownian diffusion as shown below.

All noise sources in Eq. (1) have been treated as independently tunable, although, strictly speaking, thermal and orientational fluctuations may be statistically correlated depending on the self-propulsion mechanism [5, 11, 12]. Moreover, we ignored hydrodynamic effects, which are known to favor clustering in dense mixtures of

JP's [28–30] and even cause their capture by the channel walls [31]. However, both effects are negligible for low density mixtures of pointlike spherical JP's. Moreover, we made sure that the parameters used in our simulations were experimentally accessible, as apparent on expressing times in seconds and lengths in microns and comparing with the experimental setups of Refs. [12, 20].

When confined to a channel directed along the  $x$  axis, the particle transverse coordinate,  $y$ , is bounded between a lower and upper wall,  $w_-(x) \leq y \leq w_+(x)$ , with

$$w_{\pm}(x) = \pm \frac{1}{2} \left[ \Delta + (y_L - \Delta) \sin^2 \left( \frac{\pi}{x_L} x \right) \right], \quad (2)$$

Such a sinusoidal channel is periodic; its compartments have length  $x_L$  and are mirror symmetric under both coordinate inversions,  $x \rightarrow -x$  and  $y \rightarrow -y$ , i.e., centrosymmetric. Throughout our analysis we assumed that the width,  $\Delta$ , of the pores connecting the compartments are much narrower than the maximum channel cross-section, i.e.,  $\Delta \ll y_L$ .

Simulating a constrained JP requires defining its collisional dynamics at the boundaries. For the translational velocity  $\dot{\mathbf{r}}$  we assumed elastic reflection. Regarding the coordinate  $\theta$ , we assumed that it does not change upon collision (sliding b.c. [3]). As a consequence the active particle slides along the walls for an average time of the order of  $\tau_\theta$ , until the  $\theta$  fluctuations,  $\xi_\theta(t)$ , redirect it toward the interior of the compartment. In the limit of strong persistency of the propulsion mechanism,  $l_\theta \gg x_L, y_L$ , and weak chirality,  $R_\Omega \gg l_\theta$  the stationary particle probability density  $P(x, y)$  accumulates along the boundaries; this effect is the strongest in the noiseless case,  $D_0 = 0$  [3].

The dispersion of a Brownian particle along the channel axis [32] is an important issue experimentalists address when trying to demonstrate rectification. Indeed, drift currents, no matter how weak, can be detected over an affordable observation time only if the relevant dispersion is sufficiently small. This issue is of paramount importance when one handles with active Brownian particles, like JP's, whose stochastic dynamics is characterized by strong persistency, or long correlation times. Under such conditions the current literature on classical diffusion is of little help [1, 33]. To this purpose we computed the transport diffusivity,  $D_{\text{ch}}$ , of a JP in the sinusoidal channel of Eq. (2), as the limit

$$D_{\text{ch}} = \lim_{t \rightarrow \infty} [\langle x^2(t) \rangle - \langle x(t) \rangle^2] / (2t), \quad (3)$$

which we checked to exist for all simulation parameters (normal diffusion limit).

**Bulk diffusion,  $D$ .** – An analytical solution of the model Eq. (1) is out of question even in the bulk (i.e., in the absence of boundaries) and for  $\Omega = 0$  (*nonchiral* JP). However, on noticing that [3, 30]

$$\langle \cos \theta(t) \cos \theta(0) \rangle = \langle \sin \theta(t) \sin \theta(0) \rangle = (1/2) e^{-|t|D_\theta}, \quad (4)$$

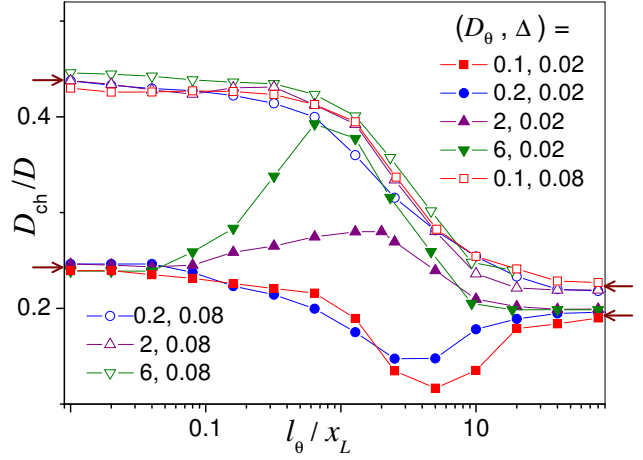


Fig. 3: (Color online) Diffusion of a nonchiral JP in the sinusoidal channel of Eq. (2):  $D_{\text{ch}}/D$  vs.  $v_0$  at constant  $D_\theta$  and  $\Delta$  (see legend).  $D$  is the bulk diffusivity of Eq. (6). Other simulation parameters are  $x_L = y_L = 1$  and  $D_0 = 0.05$ . The left and right arrows denote, respectively, the estimated values of the suppression constants,  $\kappa_0$  and  $\kappa_s$ , introduced in the text, i.e.,  $\kappa_0 = 0.25$  and  $\kappa_s = 0.20$  for  $\Delta = 0.02$ ;  $\kappa_0 = 0.45$  and  $\kappa_s = 0.23$  for  $\Delta = 0.08$ .

and the first two LE's of Eq. (1) are statistically independent, namely  $\lim_{t \rightarrow \infty} \langle \cos \theta(t) \sin \theta(t) \rangle = 0$ , one concludes immediately that a nonchiral particle diffuses according to Fürth's law

$$\begin{aligned} \langle \Delta x(t)^2 \rangle &= \langle \Delta y(t)^2 \rangle \\ &= 2(D_0 + v_0^2 \tau_\theta / 4)t + (v_0^2 \tau_\theta^2 / 2)(e^{-2t/\tau_\theta} - 1). \end{aligned} \quad (5)$$

For  $t \gg \tau_\theta$  we thus recover the asymptotic normal diffusion law,  $\langle \Delta x(t)^2 \rangle = 2Dt$ , where the constant  $D$  apparently consists of two distinct contributions,

$$D = D_0 + D_s, \quad (6)$$

due to the randomness of, respectively, the thermal fluctuations,  $D_0$ , and self-propulsion,  $D_s = v_0^2 \tau_\theta / 4$ .

Determining the  $\Omega$  dependence of the bulk diffusivity,  $D(\Omega)$ , of a chiral JP is a more challenging task. Our prediction is the phenomenological law

$$D(\Omega) = D_0 + \frac{D_s}{1 + (\Omega \tau_\theta / 2)^2}, \quad (7)$$

where  $D(0)$  coincides with  $D$  in Eq. (3). The derivation of this law can be summarized as follows: (i) As suggested by the separation between thermal and active diffusion in Eqs. (6) and (7), we focused on the limiting case of zero thermal noise,  $D_0 = 0$ ; (ii) In view of the identities in Eq. (4), we noticed that the ensuing velocity components  $\dot{x}$  and  $\dot{y}$  can be regarded as two independent non-Gaussian exponentially correlated noises with zero mean, intensity  $D_s$  and correlation time  $\tau_\theta$ ; (iii) Finally, having set  $\xi_x(t) = \xi_y(t) = 0$ , we took the time derivative of the first two LE's

in Eq. (1) and linearized them as

$$\begin{aligned}\ddot{x} &= -\Omega\dot{y} - 2\dot{x}/\tau_\theta + 2\eta(t)/\tau_\theta \\ \ddot{y} &= +\Omega\dot{x} - 2\dot{y}/\tau_\theta + 2\eta(t)/\tau_\theta,\end{aligned}\quad (8)$$

where  $\eta(t)$  denotes a stationary white Gaussian noise with zero mean and strength  $D_s$ ; (iv) From the approximate 2D stationary dynamics of Eq. (8) our prediction for  $D(\Omega)$  in Eq. (7) follows suite [34,35] (for more details see Ref. [36]).

Owing to the b.c. adopted here, for a JP diffusing in a straight channel, say, with  $w_\pm(x) = \pm y_L/2$ , bulk and channel diffusivity coincide,  $D_{\text{ch}} = D$ . This statement is confirmed by the fact that the simulation curves displayed in Fig. 2 do not depend on  $y_L$ . Most remarkably, all three curves are closely fitted by the phenomenological law (7). As expected from Eq. (7),  $D(\Omega)$  interpolates the diffusivity of a nonchiral JP, Eq. (6), at  $\Omega = 0$  and the thermal diffusivity,  $D_0$ , for  $\Omega \rightarrow \infty$ . In the latter limit, i.e., for  $R_\Omega/l_\theta \rightarrow 0$ , self-diffusion is totally suppressed.

**Channel diffusion,  $D_{\text{ch}}$ .** – When confined to a corrugated channel, the particle diffusivity is suppressed by the geometric constrictions represented by the pores, as shown in Figs. 3 and 4, respectively, for nonchiral and chiral JP's diffusing along a sinusoidal channel.

In the absence of self-propulsion, say, for  $v_0 = 0$  (or, equivalently,  $l_\theta = 0$ ), the bulk diffusivity is  $D = D_0$ , see Eq. (6), and the channel diffusivity can be written as  $D_{\text{ch}} = \kappa_0 D_0$ , with  $\kappa_0$  a well studied function of  $\Delta$  and  $D_0$  [37,38]. In the opposite limit of strong self-propulsion,  $v_0 \rightarrow \infty$ , the bulk diffusion of a *nonchiral* JP is governed by self-diffusion, that is,  $D \simeq D_s$  and, accordingly, in the channel  $D_{\text{ch}} = \kappa_s D_s$ . Both limits of  $D_{\text{ch}}$  are illustrated in Fig. 3 for different values of  $\Delta$  and  $D_\theta$ . Apparently, neither  $\kappa_0$  nor  $\kappa_s$  depend on  $D_\theta$  and both are smaller than one. This conclusion applies to different compartment geometries, symmetric and asymmetric, alike, as confirmed by further simulation results reported in Ref. [25].

The mechanisms underlying the suppression of channel diffusion quantified by the constants  $\kappa_0$  and  $\kappa_s$ , are different. For a regular Brownian particle with  $v_0 = 0$  moving in a narrow channel,  $\kappa_0$  can be estimated in Fick-Jacobs' approximation for smoothly corrugated channels [1,37] and in mean-first-exit time formalism for sharply compartmentalized channels [38,39]. In both cases,  $\kappa_0$  strongly depends on the compartment volume, the pore width and thermal noise, since particle diffusion mostly happens away from the walls. For nonchiral self-propelling microswimmers with  $l_\theta \gg x_L, y_L$ , the constant  $\kappa_s$  is mostly determined by the b.c. introduced to model the particle collisions against the channel walls. For sliding b.c., the probability flows (consequence of the JP's piling up against the boundaries [27]) are modulated by the wall profiles,  $w_\pm(x)$ , and thus not much sensitive to the pore width itself (as long as the particle size is negligible; see Ref. [25] for more details). The distinct  $\Delta$  dependence of  $\kappa_0$  and  $\kappa_s$  is apparent in Fig. 3.

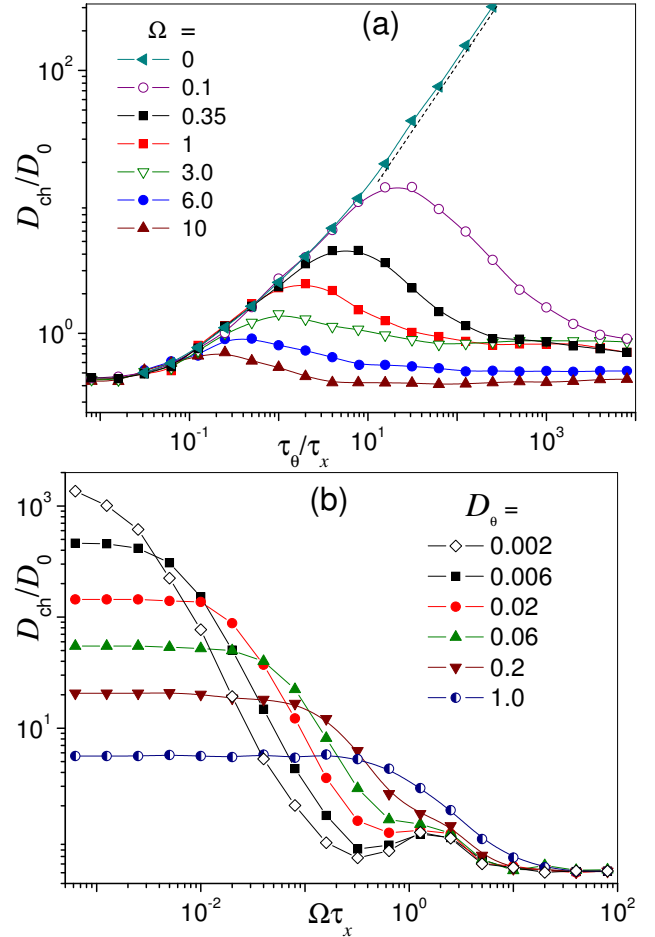


Fig. 4: (Color online) (a) Diffusion of a levogyre JP in the sinusoidal channel of Eq. (2): (a)  $D_{\text{ch}}/D_0$  vs.  $\tau_\theta$  for different  $\Omega$ . Notice that the smaller  $\Omega$ , the slower is convergence of  $D_{\text{ch}}/D_0$  to  $\kappa_0$  for large  $\tau_\theta$ ; (b)  $D_{\text{ch}}/D_0$  vs.  $\Omega$  for different  $D_\theta$ . Here,  $\tau_x \equiv x_L/v_0$ ,  $v_0 = 1$ ,  $D_0 = 0.05$ , and  $\Delta = 0.08$ . The dashed line in (a) represents the asymptotic linear power law of Eq.(6).

We consider next the case of channeled *chiral* JP's. The diffusivity of a levogyre JP's in a sinusoidal channel, illustrated in Fig. 4, clearly points to two different chirality-induced suppression mechanisms. We have already shown how chirality limits the bulk diffusion of JP's with long self-propulsion time constants, that is  $|\Omega|\tau_\theta \gg 1$  or  $R_\Omega \ll l_\theta$ , see Eq. (7). On the other hand, when the chiral radius  $R_\Omega$  grows smaller than the compartment dimensions, say,  $R_\Omega \ll x_L$ , or  $|\Omega|\tau_x \gg 1$ , all swimmers, even those with long self-propulsion length,  $l_\theta \gg x_L$ , are expected to perform closed orbits and thus get trapped inside the channel compartments [27]. Such a geometric condition is likely to produce an additional suppression of channel diffusion.

With these premises the dependence of  $D_{\text{ch}}$  on the self-propulsion mechanism parameters,  $\tau_\theta$  and  $\Omega$ , can be satisfactorily explained, at least, at a qualitative level. Curves of  $D_{\text{ch}}$  versus  $\tau_\theta$  at constant  $\Omega$  are reported in

Fig. 4(a). By inspection one notices immediately that: (i) At large  $\tau_\theta$ ,  $D_0$  is negligible with respect to  $D_s$  and, again,  $D_{\text{ch}} \simeq \kappa_s D(\Omega)$ , like for nonchiral JP's. Most remarkably, we checked that  $\kappa_s$  does not sensibly depend on  $\Omega$ ; (ii) The curves  $D_{\text{ch}}$  versus  $\tau_\theta$  go through a maximum,  $D_{\text{ch}}^{\text{max}} \simeq \kappa_s D_s/2$ , the position of which,  $|\Omega|\tau_\theta = 2$ , is insensitive to the channel geometry. Indeed, position and height of the maxima located at  $\tau_\theta > \tau_x$  can be closely approximated by plotting the bulk diffusivity of Eq. (6) as a function of  $\tau_\theta$  and making use of the relation  $D_{\text{ch}} = \kappa_s D$ ; (iii) For finite  $\Omega$ , active diffusivity in the channel is suppressed both for  $\tau_\theta \rightarrow 0$  and  $\tau_\theta \rightarrow \infty$ . In both limits, one thus expects that  $D_{\text{ch}}(\Omega) \rightarrow \kappa_0 D_0$ , where  $\kappa_0$  is the corresponding suppression constant at  $\Omega = 0$  given in Fig. 3. Note that at low  $\Omega$  the convergence toward the expected large  $\tau_\theta$  asymptote is very slow. The same asymptote is approached by the large  $\Omega$  tails of the curves plotted in Fig. 4(b).

Moreover, the  $\Omega$  dependence of  $D_{\text{ch}}$  at constant  $\tau_\theta$ , illustrated in Fig. 4(b), shows explicitly that (iv)  $D_{\text{ch}}$  starts decreasing appreciably with  $\Omega$  only for  $|\Omega|\tau_\theta \gtrsim 2$ , that is in coincidence with the maxima displayed in Fig. 4(a); (v) Small diffusivity peaks emerge for  $|\Omega|\tau_\theta \gg 1$ . They are centered around a certain value of  $\Omega$ ,  $\Omega_M$ , which does not depend on the time constant  $\tau_\theta$ .  $\Omega_M$  can be estimated by noticing that on increasing  $\Omega$  the chiral radius  $R_\Omega = v_0/|\Omega|$  decreases, until the microswimmer performs a full circular orbit inside the channel compartment, without touching its walls (actually a logarithmic spiral with exponentially small steps [17]). In the noiseless limit, this happens for  $2R_\Omega \simeq x_L$ , that is,  $\Omega_M \simeq 2v_0/x_L$ . This condition can be regarded as the onset of a mechanism of dynamical trapping. In Brownian transport theory, the onset of a trapping mechanism generally corresponds to an excess diffusion peak [40–42]: That is precisely the phenomenon we see at work here. Of course, this argument requires that  $\Omega_M \tau_\theta \gg 1$ , to ensure a sufficiently long self-propulsion time. Both our estimate for  $\Omega_M$  and the condition for the diffusivity peak to appear are in close agreement with the data displayed in Fig. 4(b).

**Conclusions.** – We numerically investigated the diffusion of artificial active microswimmers moving along narrow periodically corrugated channels. Our work is meant to complement the earlier literature on the rectification of active microswimmers in confined geometries. Transport quantifiers, like rectification power and diffusivity, strongly depend on the particle self-propulsion mechanism and the channel compartment geometry. The emerging picture suggests the possibility of developing new control techniques for the manipulation of artificial microswimmers, which are well within the reach of today's technology. Specialized microfluidic circuits can be designed, for instance, to guide chiral microswimmers to a designated target. The same technique can be utilized to fabricate monodisperse chiral microswimmers (presently a challenging technological task). By the same token, mi-

croswimmers capable of inverting chirality upon binding to a load, can operate as chiral shuttles along a suitably corrugated channel even in the absence of gradients of any kind.

\*\*\*

X.A. has been supported by the grant Equal Opportunity for Women in Research and Teaching of the Augsburg University. P.H. and G.S. acknowledge support from the cluster of excellence Nanosystems Initiative Munich (NIM). Y.L. was supported by the NSF China under grants No. 11347216 and 11334007, and by Tongji University under grant No. 2013KJ025. F.M. thanks the Alexander von Humboldt Stiftung for a Research Award.

## REFERENCES

- [1] BURADA P. S., HÄNGGI P., MARCHESONI F., SCHMID G. and TALKNER P., for a review see, *ChemPhysChem*, **10** (2009) 45.
- [2] HÄNGGI P. and MARCHESONI F., *Rev. Mod. Phys.*, **81** (2009) 387.
- [3] GHOSH P. K., MISKO V. R., MARCHESONI F. and NORI F., *Phys. Rev. Lett.*, **110** (2013) 268301.
- [4] PURCELL E. M., *Am. J. Phys.*, **45** (1977) 3.
- [5] SCHWEITZER F., *Brownian Agents and Active Particles* (Springer, Berlin Heidelberg) 2003.
- [6] RAMASWAMY S., *Annu. Rev. Condens. Matter Phys.*, **1** (2010) 323.
- [7] VICSEK T. and ZAFEIRIS A., *Phys. Rep.*, **517** (2012) 71.
- [8] ROMANCZUK P., BÄR M., EBELING W., LINDNER B. and SCHIMANSKY-GEIER L., *Eur. Phys. J. Special Topics*, **202** (2012) 1.
- [9] JIANG S. and GRANICK S. (Editors), *Janus Particle Synthesis, Self-Assembly and Applications* (RSC Publishing, Cambridge) 2012.
- [10] WALTHER A. and MÜLLER A. H. E., *Chem. Rev.*, **113** (2013) 5194.
- [11] PAXTON W. F., SUNDARARAJAN S., MALLOUK T. E. and SEN A., *Angew. Chem. Int. Ed.*, **45** (2006) 5420.
- [12] VOLPE G., BUTTINONI I., VOGT D., KÜMMERER H.-J. and BECHINGER C., *Soft Matter*, **7** (2011) 8810.
- [13] JIANG H. R., YOSHINAGA N. and SANO M., *Phys. Rev. Lett.*, **105** (2010) 268302.
- [14] BARABAN L., STREUBEL R., MAKAROV D., HAN L., KARNAUSHENKO D., SCHMIDT O. G. and CUNIBERTI G., *ACS Nano*, **7** (2013) 1360.
- [15] HONG Y., VELEGOL D., CHATURVEDI N. and SEN A., *Phys. Chem. Chem. Phys.*, **12** (2010) 1823.
- [16] BÚZÁS A., KELEMEN L., MATHESZ A., OROSZI L., VIZSNYICZAI G., VICSEK T. and ORMOS P., *Appl. Phys. Lett.*, **101** (2012) 041111.
- [17] VAN TEEFFELN S. and LÖWEN H., *Phys. Rev. E*, **78** (2008) 020101.
- [18] FRIEDRICH B. M. and JÜLICHER F., *Phys. Rev. Lett.*, **103** (2009) 068102.
- [19] BROKAW C. J., *J. Exp. Biol.*, **35** (1958) 97. *J. Cell. Comp. Physiol.*, **54** (1959) 95.
- [20] MIJALKOV M. and VOLPE G., *Soft Matter*, **9** (2013) 6376.

- [21] KÜMMEL F., TEN HAGEN B., WITTKOWSKI R., BUTTINONI I., EICHHORN R., VOLPE G., LÖWEN H. and BECHINGER C., *Phys. Rev. Lett.*, **110** (2013) 198302.
- [22] BOYMELGREEN A., YOSSIFON G., PARK S. and MILOH T., *Phys. Rev. E*, **89** (2014) 011003(R).
- [23] SEN A., IBELE M., HONG Y. and VELEGOL D., *Faraday Discuss.*, **143** (2009) 15.
- [24] ZÖTTL A. and STARK H., *Phys. Rev. Lett.*, **108** (2012) 218104.
- [25] AO X., GHOSH P. K., LI Y., SCHMID G., HÄNGGI P. and MARCHESONI F., *Eur. Phys. J Special Topics*, **223** (2014) 3227.
- [26] TEN HAGEN B., VAN TEEFFELEN S. and LÖWEN H., *J. Phys.: Condens. Matter*, **23** (2011) 194119.
- [27] LI Y., GHOSH P. K., MARCHESONI F. and LI B., *Phys. Rev. E*, **90** (2014) 062301.
- [28] RIPOLL M., HOLMQVIST P., WINKLER R. G., GOMPPER G., DHONT J. K. G. and LETTINGA M. P., *Phys. Rev. Lett.*, **101** (2008) 168302.
- [29] BUTTINONI I., BIALKÈ J., KÜMMEL F., LÖWEN H., BECHINGER C. and SPECK T., *Phys. Rev. Lett.*, **110** (2013) 238301.
- [30] FILY Y. and MARCHETTI M. C., *Phys. Rev. Lett.*, **108** (2012) 235702.
- [31] TAKAGI D., PALACCI J., BRAUNSCHWEIG A. B., SHELLEY M. J. and ZHANG J., *Soft Matter*, **10** (2014) 1784.
- [32] MACHURA L., KOSTUR M., TALKNER P., LUCZKA J., MARCHESONI F. and HÄNGGI P., *Phys. Rev. E*, **70** (2004) 061105.
- [33] BRENNER H. and EDWARDS D. A., *Macrotransport Processes* (Butterworth-Heinemann, New York) 1993.
- [34] TAYLOR J. B., *Phys. Rev. Lett.*, **6** (1961) 262.
- [35] KURŞUNOĞLU B., *Phys. Rev.*, **132** (1963) 21.
- [36] Ao X., PhD thesis (Augsburg University, in preparation).
- [37] BURADA P. S., SCHMID G., REGUERA D., RUBI J. M. and HÄNGGI P., *Phys. Rev. E*, **75** (2007) 051111.
- [38] BOSI L., GHOSH P. K. and MARCHESONI F., *J. Chem. Phys.*, **137** (2012) 174110.
- [39] BORROMEO M. and MARCHESONI F., *Chem. Phys.*, **375** (2010) 536.
- [40] SCHREIER M., HÄNGGI P. and POLLAK E., *Europhys. Lett.*, **44** (1998) 416.
- [41] COSTANTINI G. and MARCHESONI F., *Europhys. Lett.*, **48** (1999) 491.
- [42] REIMANN P., VAN DEN BROEK C., LINKE H., HÄNGGI P., RUBÍ J. M. and PEREZ MADRID A., *Phys. Rev. Lett.*, **87** (2001) 010602.